Vision Res. Vol. 22, pp. 1313 to 1328, 1982
Printed in Great Britain

0042-6989/82/101313-16$03.00/0
Pergamon Press Ltd

THE DELAYED ROD AFTERIMAGE

EDWARD H. ADELSON*
Vision Research Laboratory, University of Michigan, Department of Psychology, Ann Arbor, MI 48109, U.S.A.

(*Received* 16 *July* 1981; *in revised form* 5 *March* 1982)

Abstract—A flashed background, presented to a dark-adapted eye, can saturate the rod system, making an incremental test patch invisible. But as the afterimage decays, the test can be distinguished. Increment thresholds measured within the decaying afterimage exhibit Weber's law over a wide range. The Penn and Hagins model of rod kinetics correctly predicts Weber's law, but makes incorrect predictions of the latency for the detection to occur. A new model, involving two exponential decays, is able to accommodate the latency data, as well as Weber's law. The model also makes good predictions of the results when the stimulus duration is increased from 100 msec to 1 sec.

INTRODUCTION

The positive afterimages that ensue after a brief flash of light can be quite striking. Here is a description from Duke-Elder (1934):

"... If the eyes are turned towards a spot of light, yet protected from it by a card, if this card is rapidly removed and as rapidly replaced, the light is seen as a positive homochromatic afterimage with all its original brightness and detail. So vivid, indeed, may be the impression of the original afterimage that the card appears transparent, and details which were not noted in looking at the light are brought to the attention in the afterimage."

This last effect, the improved discrimination in the afterimage, was also noted by Helmholtz (1924):

"... when a lamp with a round wick is quickly extinguished, by watching the flame vanish, we can see by the afterimage that the flame was brighter at the edges than in the middle; although it is hard to see this by looking directly at the flame itself."

Brindley (1959) seems to have been the first to make quantitative measurement on the discrimination of lights by their afterimages, for lights that were initially indistinguishable. He was interested in the long-lasting negative afterimages that follow very bright flashes. MacLeod, Hayhoe, and their colleagues (MacLeod and Hayhoe, 1974; Hayhoe *et al.*, 1976; Gosline *et al.*, 1976) extended this approach in a beautiful series of experiments on rod afterimages—again concentrating on the long-lasting effects of very bright flashes, and the negative afterimages associated with them.

But the afterimages described in the above passages from Duke-Elder and Helmholtz are of a different sort. They are positive, relatively short, and are produced by lights that bleach very small amounts of pigment. The experiments that follow deal with these afterimages.

The present work has its beginnings in an observation by Sakitt (1976), who had saturated the rod system of a rod monochromat, using a bright, steady adapting field. Against this background, the monochromat could never distinguish a test flash, no matter how bright. However, if she closed her eyes immediately after the flash was presented, she could make out the test in the positive afterimage.

As Sakitt pointed out, this implied that the test flash was producing a lasting effect at some point *distal* to the saturating bottleneck. If, as some believe, rod saturation occurs at the level of the rod itself, then the rod afterimage must have reflected the accumulation and decay of some substance (or effect) within the rod outer segment.

At about the same time, Geisler (1975) made some related observations in cones. Cones cannot normally be saturated with steady lights, and Geisler was using flashed backgrounds to produce the saturation, following the technique introduced by Alpern *et al.* (1970b). Above some intensity, he indeed found that cone increment thresholds began to take a sharp upward turn; but he also noticed that he could make discriminations quite easily using the positive afterimage rather than the initial image.

The present experiments involve rods (in normal subjects) and use the flashed background technique to produce transient rod saturation, as described elsewhere (Adelson, 1977a; 1982). This technique produces dramatic positive rod afterimages, within which one can discriminate differences that were quite invisible in the initial image. Because saturation occurs at lower light levels than it would in the steady state, cone intrusion is less of a problem, and one can follow the behavior of rod afterimages over a large range of background flash intensities.

Stimuli generally consisted of a green test on a red background. The background and test were presented

*Present address: RCA, David Sarnoff Research Center, Princeton, NJ 08540, U.S.A.

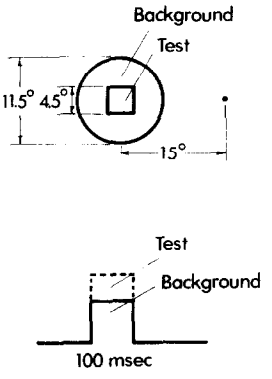

Fig. 1. Typical stimulus conditions for producing the delayed rod afterimage. The test was green (Ilford No. 624), while the background was red-orange (Wratten No. 24). Both test and background were flashed simultaneously to a dark-adapted eye for 100 msec.

simultaneously in a 100 msec flash (see Fig. 1). Typical impressions that would follow these background-test presentations are shown in Fig. 2. Time proceeds to the right; the three rows represent the impressions following three successively brighter background flashes, where the simultaneous test flash was bright enough to produce an easily discriminable afterimage.

In the top row is the impression at low light levels: the subject can see the test immediately in the presentation. The second row shows the impression following a background and test of intermediate intensity: during the presentation itself (first disc), the rod system is saturated, and so the test is indistinguishable from the background. But as the eye is immediately returned to darkness, the glowing positive afterimage shows the test clearly, after a few hundred milliseconds. The bottom row shows that after a very bright flash, it may take several seconds before the test becomes discriminable amidst the decaying afterimage.

The actual visual impressions are more complex than shown in Fig. 2. The initial flash produces a sensation of great brightness; the offset of the flash gives a dramatic drop in brightness; and this is followed by the slower waxing and waning of the positive afterimage. Sometimes the afterimage as a whole seems to become brighter as the test emerges from within it. The sequence of impressions is produced by a complex chain of events beginning with both rods and cones (cones can respond to the background, even if they are prevented from detecting the test) and traversing the entire visual system. I will not attempt to quantify the complete phenomenology, but instead will ask the following, simpler, question: what process or processes underlie the discrimination of the test region in the delayed positive afterimage?

The Penn and Hagins model

Sakitt (1976) pointed out that her effects could be produced by a system built along the lines of the Penn and Hagins (1972) model. Sakitt modified the Penn and Hagins scheme, but her modifications will not be discussed here, since the original scheme actually does a better job of explaining the afterimage effects. The model proposed by Penn and Hagins is shown in Fig. 3.

Penn and Hagins found that the photocurrent of the rod outer segment grew linearly with the intensity of the stimulating flash, until it approached a saturating ceiling. In the linear range, the impulse response could be modelled with a string of four simple low-pass stages, with each stage contributing a single pole. The output of the system then goes through a saturating stage of the form

$$V_{out} = \frac{H}{(H + \sigma)} \tag{1}$$

where V_{out} is the output of the saturating stage, σ is the semisaturation constant, and $H = H(t)$ is the response of the linear system preceding saturation.

The physiology underlying the model merits a brief description, even though it is not essential to the modelling of afterimages. The absorption of quanta in the rod outer segment leads, through a series of chemical reactions, to the production of some internal transmitter substance. The kinetics of the production and decay of this substance are modelled by the string of low-pass filters. The transmitter blocks the flow of sodium ions through the outer segment membrane. When the sodium channels are completely blocked, the sodium current is as small as it can be (and, by a sign inversion, the photoresponse is as large as it can be). This complete blocking represents rod saturation.

The Penn and Hagins model leads directly to a prediction of the delayed rod afterimage effect, as illustrated in the bottom panels of Fig. 3. On the left are shown the *internal* responses to two different intensities of light—let us say, the intensities of the background and test regions. The internal responses are linear. But the output is compressed by the saturating ceiling, as shown on the right (rescaled for clar-

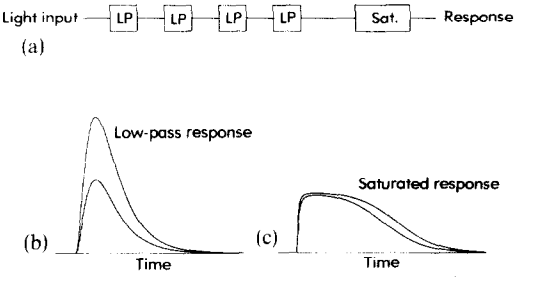

Fig. 3. The Penn and Hagins model of rod response and rod saturation; (a) a string of low-pass filter stages generates a linear response, which is than compressed by a hyperbolic saturation; (b) the internal response to two flashes of different intensity; (c) the same responses after passing through the saturating stage (rescaled for clarity). The responses are indistinguishable while they are compressed against the saturating ceiling, but become distinguishable when they decay below saturation.

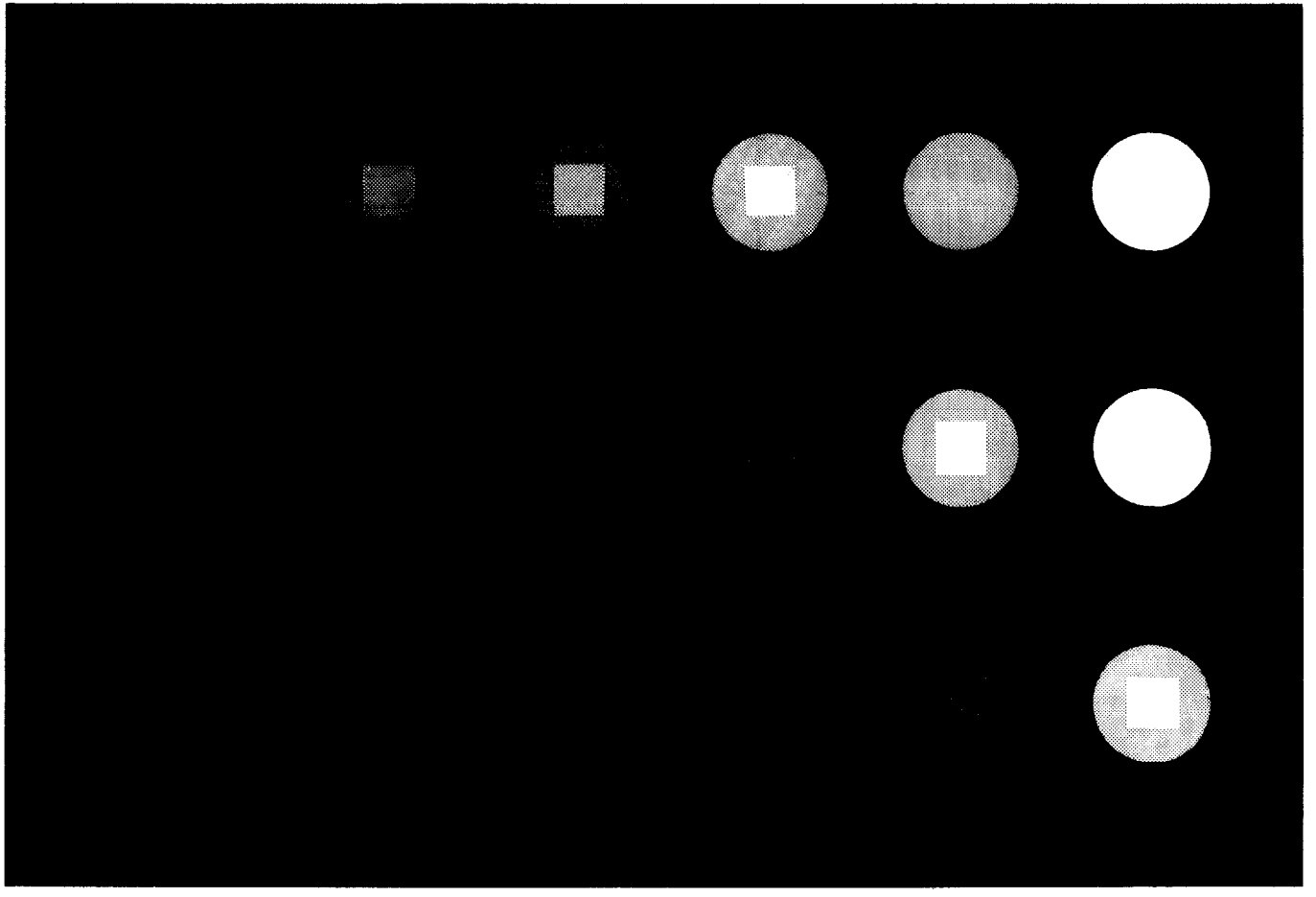

Fig. 2. The subjective impressions following the presentation of a 100 msec background and simultaneous test flash. Time proceeds to the right. Top: when the flash intensities are low, the test is immediately discriminable. Middle: when the flash intensities are increased, the test is initially invisible, due to saturation, and only becomes visible in the positive afterimage which follows. Bottom: with brighter flashes, the afterimage remains saturated for a longer time, before finally decaying to the point where the test is visible.

ity). Both outputs are initially compressed against the ceiling, and so are indistinguishable from each other. Only after they have decayed into the linear region can their difference be distinguished. Thus, while the test patch is initially invisible, it does show itself clearly in the afterimage.

This style of model, with appropriate modifications, can be used to explain a great deal of the data. One must keep in mind, of course, that the inferences are functional rather than physiological, and that the data may or may not reflect processes occurring at the receptor level.

One further comment is in order here. The Penn and Hagins model involves no adaptation, and indeed most of the models that will be discussed assume non-adapting systems. There is evidence that the rod system does show adaptation in conditions similar to those used here (Adelson, 1982), but those effects will be ignored for the moment. Two apologies may be offered for this approach: first, the non-adapting models are much easier to analyze mathematically, and turn out to be sufficiently strong to account for most of the data; and second, it will be shown that the effects of adaptation will modify, but not severely disrupt, the main inferences based on the non-adapting models.

EXPERIMENT 1. ACTION SPECTRUM FOR AFTERIMAGES

The first task is to make sure that the positive afterimage effects of Fig. 2 actually reflect rod signals. A test sensitivity and field sensitivity were run on afterimage discrimination, to check whether they would show scotopic action spectra.

Methods

The apparatus was a 2 channel Maxwellian view system, described in detail in Adelson (1982). The test was a 4.5° square, presented against an 11° circular background. The stimulus was presented 12° nasal from the fixation point. Test light entered the pupil through the nasal edge, while the background light entered through the center.

For the test sensitivity, a red-orange background (Wratten No. 24, scotopic mean wavelength 603) of 3.2 log scot. td was flashed to a dark adapted eye for 100 msec. The test patch, which was of varying wavelength (selected by interference filters) was superimposed simultaneously for the 100 msec. On successive trials, the subject adjusted the intensity of the test patch until it was just visible when it appeared in the afterimage.

For the field sensitivity, the test was always green (Ilford No. 624, scotopic mean wavelength 527 nm), at 2.7 log scot. td. The background beam was varied in wavelength, and the subject adjusted the background's intensity on successive trials, until it was at the intensity which left the test just discriminable in the afterimage.

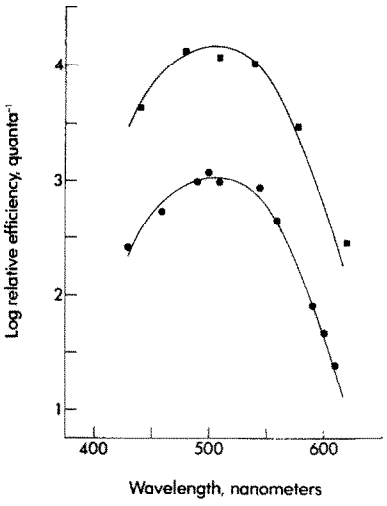

Fig. 4. Action spectra for delayed afterimage production. Top: test sensitivity. The red-orange background was fixed at an intensity of 3.2 log scot. td; the test wavelength was varied; and the test intensity was adjusted for threshold in the afterimage. Bottom: field sensitivity. The green test was fixed at an intensity of 2.7 log scot. td; the background wavelength was varied; and the background intensity was adjusted to cause the test to be at threshold in the afterimage. The smooth curves are the quantized CIE scotopic luminosity function, slid vertically to fit the data. Subject E.A.

Results

Figure 4 shows the results. The test sensitivity is shown in the upper curve (squares); the field sensitivity (circles) is below. The solid line in each case is the quantized CIE scotopic luminosity function, slid vertically to fit the data. The fit is fairly good in both cases, indicating that the afterimage discrimination is determined by rod signals.

EXPERIMENT 2. STILES–CRAWFORD EFFECT

The Stiles–Crawford effect offers another way of testing whether rods alone are responsible for discrimination in the delayed afterimage discrimination. Since rods have little or no directional sensitivity, afterimage discrimination should not depend on the point of pupillary entry.

Methods

The 100 msec test was green (Ilford No. 624); the 100 msec background was red-orange (Wratten No. 24). The background was 3.2 log scot. td, and entered the eye through the center of the pupil. The test's entry point was varied, and its intensity was adjusted for threshold in the afterimage.

Results

The resulting directional sensitivity curve, shown in Fig. 5, is essentially flat, as one would expect if rods were making the discrimination. As a control, this

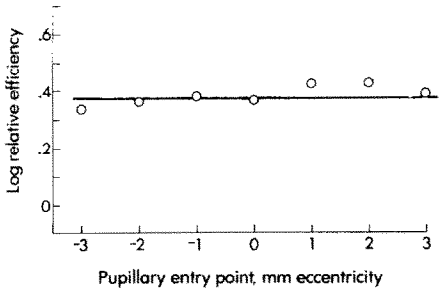

Fig. 5. Stiles–Crawford effect for the delayed afterimage. Test pupillary entry point was varied, and the test intensity was adjusted for threshold in the afterimage. Positive eccentricity is nasal; negative is temporal. Subject E.A.

same subject's Stiles–Crawford effect was measured for the cones in the same region of the retina. For this purpose, the test was made red-orange, and the background green (2.1 log scot. td). Test threshold was measured as test pupil entry point was varied. A clear Stiles–Crawford effect was observed, which, on a logarithmic plot, could be described by a parabola of form $-pd^2$, where $p = 0.03$, and d is eccentricity in mm.

Predictions from the Penn and Hagins model

The Penn and Hagins model of rod response allows one to make some quantitative predictions about the delayed afterimage discrimination. Figure 6(a) shows the output of a computer simulation of the responses of such a system to a set of light flashes of increasing intensity. The kinetics of the system shown are taken directly from Penn and Hagins' (1972) model of the response of rat rods at 36°C.

Above are shown the responses as the inputs are increased in 0.5 log unit steps. As the inputs become larger, the responses saturate, and so cannot increase in amplitude. However, the response durations *do* continue to increase.

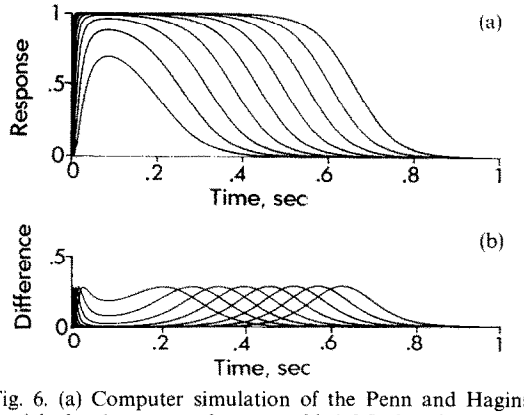

Fig. 6. (a) Computer simulation of the Penn and Hagins model of rod response, for a set of brief flashes, increasing in intensity by 0.5 log unit steps. (b) The "difference responses", computed as the arithmetic difference between each adjacent pair of responses above.

Now suppose that one input represents a background flash, and that the next brighter input represents the stimulus in the test region. Any pair of adjacent responses in Fig. 6(a) can be taken to represent the response to the background and to the test regions, for a given condition. If one follows this adjacent pair of responses, one finds that they are indistinguishable for some period of time, but then cleanly separate as they decay below saturation.

Below, in Fig. 6(b), are shown the arithmetic differences between any two adjacent responses shown in Fig. 6(a). These curves represent "difference responses", and can be taken to indicate how distinguishable the background and test regions will be in the afterimage. After a certain period of indistinguishability, the difference response rises, peaks, and falls. This behavior is consistent with the phenomenology of the afterimages.

There are two major quantitative predictions that emerge from the difference response curves. The first prediction derives from the fact that the differences always reach a fixed peak height, as long as the input pairs are always in a fixed ratio, as they are here (0.5 log unit in this case). Thus, if the background and test flashes are in a given ratio, the delayed afterimages will have a given discriminability, regardless of the absolute intensities of the background and test. In other words, Weber's law should hold for increment thresholds involving afterimage discrimination.

The second prediction is that the peak of the difference response—the moment of maximum discriminability—should occur at later and later times, and that this time should increase in a simple and orderly fashion. The increase should be nearly linear with the log of the flash intensity, at a rate of about 575 msec per log unit.

Each of these predictions was tested in the experiments that follow.

EXPERIMENT 3. INCREMENT THRESHOLDS

For a given background intensity, it is possible, over successive trials, to find the test intensity which causes the test patch to become just discriminable, when it emerges in the afterimage. In the following experiment, increment thresholds were actually measured over the entire range of background intensities available, starting at absolute threshold. At low background intensities, discriminations were made in the initial image and afterimages played no role. As the backgrounds became brighter, discrimination became easier in the afterimage than in the initial image, and the subjects switched over to this mode of discrimination. The dividing line between image and afterimage is not always well defined: subjectively, one does not have the sense of a discrete switching from one mode to the other. Referring back to Fig. 2, one finds that the test becomes visible at later and later moments as flash intensity increases.

Methods

As before, the test was green (Ilford No. 624) and the background was red-orange (Wratten No. 24); both were flashed simultaneously for 100 msec to a dark adapted eye. Over repeated trials, the subject adjusted the test intensity until it was just discriminable, using the image or the afterimage, whichever gave lower threshold.

Above 3 log scot. td-sec, it was necessary to remove the colored filters in order to allow more light through. Since this made the test visible to the cones initially, the subject was instructed to make the discrimination in the afterimage only. This caused no difficulty, since at these light levels the afterimage was quite delayed.

Between trials, the subject waited in the dark until all traces of afterimages were gone.

Results

Figure 7 shows the results for two subjects. Data for C.L. (open circles) have been shifted up 2 log units. When the background flashes were below about 0 log scot. td-sec, the discriminations were made using the initial image. Subject E.A. showed a slope near unity; subject C.L. showed a slope near 0.7.

Above about 1 log scot. td-sec, discrimination occurred in the afterimage. For both subjects, over a range of about 3 log units, afterimage discrimination fell nearly on the Weber line of unit slope. At still higher intensities, the thresholds began to rise above this line.

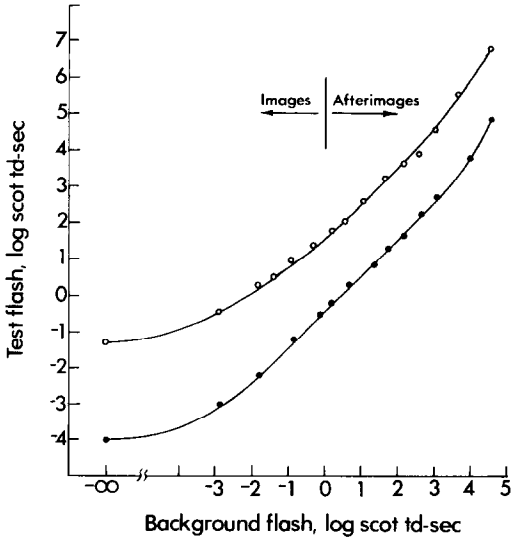

Fig. 7. Increment thresholds, with rod isolation technique, for 100 msec flashes of background and test. Data for subject C.L. (open circles) have been shifted up 2 log units. Above about 1 log scot. td-sec, subjects began making discriminations in the afterimage, rather than in the initial image (the transition is not sharp). Both subjects show Weber's law for afterimage discrimination over about 3 log units; the data deviate somewhat at the highest intensities.

No significant amount of rhodopsin was bleached in these experiments. At 4.6 log scot. td-sec, the brightest flash used, less than 1% of the rhodopsin should be bleached (Alpern, 1971).

Weber's law—the constancy of the test to background ratio—shows itself as a 45° slope on log-log coordinates. As predicted by the Penn and Hagins model, the afterimages display Weber's law over several log units of intensity.

EXPERIMENT 4. AFTERIMAGE LATENCIES

When the test patch becomes visible in the afterimage, it seems to appear and disappear in a short time. There is some instant at which it is strongest, and then it decays. If the test flash is slightly above threshold for afterimage detection, the subject can judge the time at which the test afterimage reaches its brief peak.

The Penn and Hagins model leads to the prediction that this latency should increase almost linearly with the logarithm of stimulus intensity.

Methods

The subject was shown a green test on a red-orange background, both of which were flashed for 100 msec, as in Experiment 3. For a given background intensity, the subject adjusted the test for threshold in the afterimage. Next, a 0.1 log unit neutral density filter was removed from the test beam, so that the test was 0.1 log unit above threshold. This slight increase in intensity made the emergence of the test in the afterimage a clear event, so that the subject could easily time it.

Timing was done in one of two ways. In the first procedure, the stimulus was triggered in synchrony with an electronic metronome, and the subject adjusted the metronome rate on successive trials so that one of the clicks coincided with the appearance of the test. The clicks were counted and the total time computed. In the other procedure, a single auditory tone occurred after a variable delay, and the subject adjusted the delay until the tone coincided with the appearance of the test. Both procedures gave similar results.

Results

The afterimage latencies for 3 subjects are plotted in Fig. 8, with log background flash intensity along the abscissa. The dashed line shows the prediction from the Penn and Hagins model. While it works well at low intensities, it fails badly at the higher intensities; the actual afterimage latencies become much longer than predicted by the model.

Discussion

While the Penn and Hagins model correctly predicts Weber's law for afterimage discrimination, it makes a bad prediction on the latencies. It appears

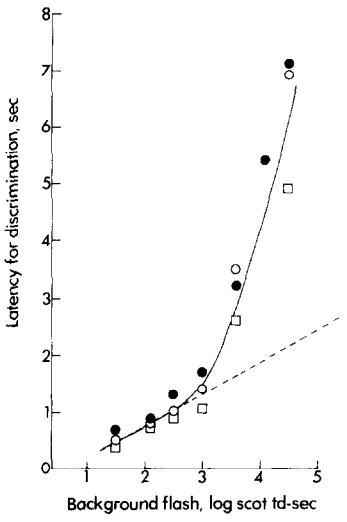

Fig. 8. Latency for the test to become visible in the afterimage, when it is 0.1 log unit above threshold. Data for 3 subjects. Dashed curve: prediction based on Penn and Hagins model. Solid curve: prediction from double exponential model (discussed later in text).

that the time constants underlying afterimage decay become rather slow at the higher flash intensities, causing the latencies to become increasingly long.

Interestingly enough, just this sort of slowing down has been observed in the electrophysiology. Penn and Hagins observed it themselves, and remarked that their model began to fail for flashes substantially above saturation; this failure took the form of an apparent increase in the time constant of decay.

IMPROVED MODELS

The slowing down of the decay after bright flashes appears necessary to explain the afterimage latencies. The Penn and Hagins model cannot give such an effect, because its decay is virtually that of a single exponential for times beyond 300 msec or so, and thus always exhibits the same time constant for afterimage decay.

Baylor *et al.* (1974) found that turtle cones displayed the slowed decay effect, and they proposed some biochemical kinetics that could account for it. Suppose that the internal transmitter—the "blocking particle", as they call it—decays into a sequence of other products, and that back reactions from the later products can hold up the decay of the transmitter when their concentration becomes large. If the later stages in this cascade are slower than the earlier ones, then the blocking particle will not decay as a single exponential, but rather as a sequence of successively slower exponentials, as the blocking particle is held up behind the later reactions (Note: Baylor *et al.* also used a non-linear autocatalytic reaction to account for adaptational effects. These nonlinear processes will be avoided for the present.)

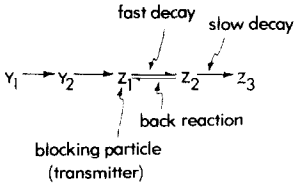

Fig. 9. Kinetics for the production and degradation of the rod response, adapted from part of the model of Baylor *et al.* See text for details.

A simple model, based on this kind of reaction, is shown in Fig. 9. The blocking particle, Z_1, is produced by a chain of reactions (Y_1 and Y_2), and broken down through another chain of reactions (Z_2 and Z_3). The concentration of Z_1 leads to an output voltage through a hyperbolic saturation. This model was applied to afterimages by Adelson (1979); Geisler (1980) has used a similar model.

A computer simulation of this model is shown in Fig. 10. The parameters have been chosen to give a reasonable prediction of the afterimage data. In the top half are shown the responses to inputs which increase in intensity in 0.5 log unit steps; below are shown the arithmetic differences between adjacent response pairs. If these are interpreted in terms of afterimages, two predictions can be made. First, Weber's law will hold for afterimage discrimination, since the difference responses all reach the same peak when the input pairs are in a fixed ratio. Second, the latencies for afterimage discrimination will grow at an accelerated rate for fixed log increments in intensity. In other words, the latency data should curve upwards, just as they actually did in Experiment 4 (Fig. 8).

It is possible, by choosing appropriate rate constants for the decay process, to produce very good fits to the afterimage latency data, and at the same time preserve Weber's law for detection. Figure 11 shows the fits to the latency data that are possible for appropriately chosen parameters; each subject has been fit individually. The time constants for subject C.L. are 160 msec and 1.24 sec; for A.B. they are 200 msec and 1.70 sec; for E.A. they are 200 msec and 1.74 sec.

The data points marked "WG" were taken from Geisler (1980), and show the results he obtained in

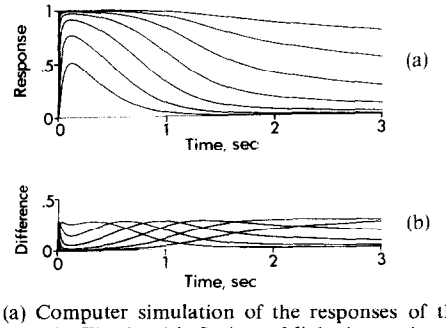

Fig. 10. (a) Computer simulation of the responses of the model shown in Fig. 9, with flashes of light increasing in 0.5 log unit steps. (b) Difference responses computed from adjacent responses above.

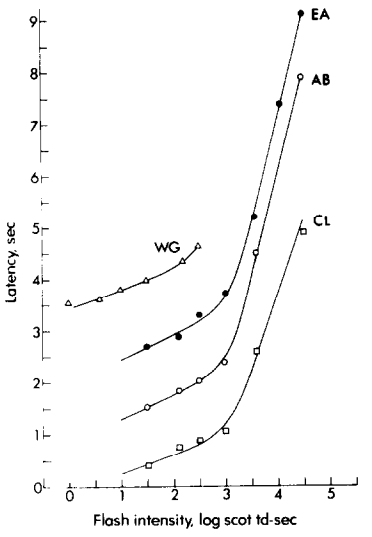

Fig. 11. Fits of the double exponential model to the latency data of Fig. 8. Subjects A.B. and E.A. have been shifted upward by 1 and 2 sec respectively. The data prints labeled "WG" are taken from Geisler (1980), and are shifted upward by 3 sec. Parameters for each subject were adjusted individually.

similar (but not identical) conditions. Geisler used reaction time to measure latency, adjusted the test to be 0.3 log units above threshold, and used test and background flashes of 50 msec. Geisler's measurements begin at a lower intensity than do the present ones, but they stop short of the high intensity leg. In the overlapping region, the results are quite similar. The solid curve through Geisler's data is generated by the double exponential model with time constants of 160 msec and 1.2 sec, time constants that are similar to those obtained for the other subjects in Fig. 11. Adding a third stage to the cascade—such as the 70 msec stage suggested by Geisler—would improve the fit at the lowest intensities, although the fit is fairly good as it stands.

It is encouraging to know that a relatively simple model is capable of fitting the data, but one would like to know how unique this particular model is. To answer this question, one must turn to the mathematics underlying afterimage discrimination, and in particular to two theorems that are proved in the appendix.

The first theorem states that any linear system followed by a fixed saturation and discrimination will result in Weber's law for afterimage discrimination. When, for example, the Penn and Hagins model was used to predict afterimage phenomena, the linear system consisted of a string of low-pass filters, the saturation was hyperbolic, and the discrimination depended on the peak of the arithmetic difference response. But almost any linear system, any saturation, and any reasonable discrimination function, will predict Weber's law as well, as long as the saturation and discrimination are independent of time.

The second theorem states that, given a system of the sort just described, the afterimage latencies will be entirely determined by the impulse response of the linear system, and will be entirely unaffected by the particular choice of saturation or discrimination function (except for a scaling on the intensity axis). Conversely, with such a system, the latency data completely define the decay of the linear system's impulse response, up to a scaling. In fact, if one rotates the latency data 90° clockwise, and relabels the axes as "log response" vs "time" one directly produces a picture of the linear system's impulse response. This is illustrated in Fig. 12. In practice, one can only gather data on the falling portion of the curve, so one can only give a rough guess about the rising phase of the response (shown in Fig. 12 with dashed lines).

It now will become clear why the model based on the Baylor *et al.* kinetics is able to fit the data. The particular choice of saturation and discrimination function matter not at all. Indeed, the chemical kinetics themselves are not terribly special. What is crucial is that this model uses a *linear* system, and

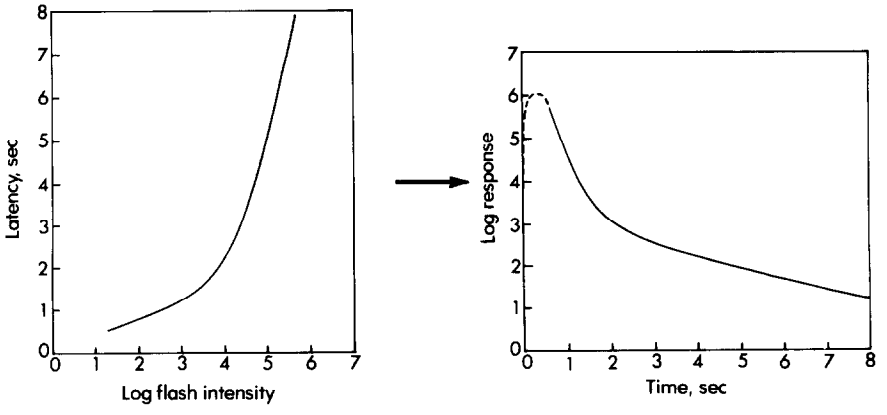

Fig. 12. The relationship between the latency data and the underlying impulse response, according to theorem 2: they are related by a rotation and a simple relabelling of axes.

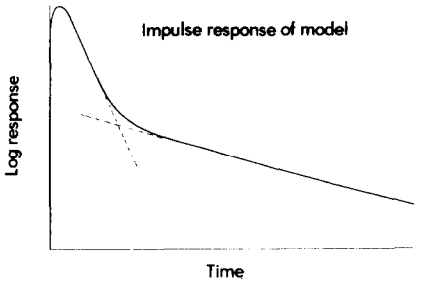

Fig. 13. The impulse response of the system with double exponential decay. On a semi-log plot, the decay curve is the envelope of two straight lines, with a smooth transition at the intersection. The curve passes 0.3 log unit above the intersection point.

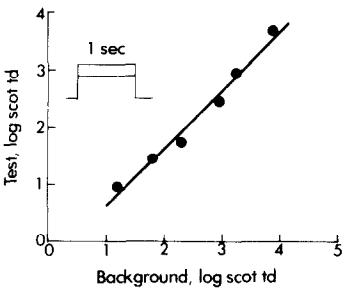

Fig. 14. Increment thresholds for afterimage discrimination, with long flashes. Rod isolation conditions. Background and test both lasted 1 sec. Subject E.A.

that the impuse response can be arranged to have the same shape as the latency data. Since the latency data tend to fall on two straight lines (on a semi-log plot), they can be modelled by a system whose impulse response is the sum of two exponentials. And the Z_1, Z_2, Z_3 cascade, which determines the shape of the decay portion of the impulse response, leads, in fact, to a double exponential decay, as shown in Fig. 13. Any model whose impulse response is similar in shape will predict the latency data just as well. And, by theorem 2, it will also predict Weber's law as long as it is linear before the saturation.

Experiments with long flashes

The double exponential model of afterimage decay leads to some predictions. First of all, in theorem 1, a linear system followed by fixed saturation and discrimination should give Weber's law regardless of the input waveform (see the appendix). Thus, if both the test and background flashes are extended to last 1 sec, rather than 100 msec, Weber's law should continue to hold. This is tested in the next experiment.

EXPERIMENT 5. THRESHOLDS WITH LONG FLASHES

Methods

The conditions were essentially the same as in Experiment 3, except that now both the test and background flashes lasted 1 sec. The test was green (Ilford No. 624), and the background was red-orange (Wratten No. 24). The measurements were only taken over the region where discrimination was clearly in the afterimage, rather than in the initial image.

Results

Figure 14 shows the afterimage increment thresholds for the 1 sec flashes. Weber's law holds fairly well, as predicted, over the nearly 3 log unit range tested.

The Weber's law result is consistent with the double exponential model, but it is also consistent with any model that incorporates a linear system preceding a fixed saturation. A more telling test of the model is to predict the latencies following long or short flashes. If the impulse response is really a double exponential, the latency curve will change in a predictable way when the flash duration is extended.

EXPERIMENT 6. LATENCIES WITH LONG FLASHES

A single stage with an exponential impulse response will give the following response to a unit step

$$V = 1 - \exp(-t/\tau) \tag{2}$$

and thus the response at the end of a step of duration T will be

$$V = 1 - \exp(-T/\tau) \tag{3}$$

Now, when the input duration is increased from 100 msec to 1 sec, the response at the termination of the input will increase by the ratio

$$\frac{V(1)}{V(0.1)} = \frac{1 - \exp(-1/\tau)}{1 - \exp(-0.1/\tau)}. \tag{4}$$

Suppose, for example, that $\tau_1 = 250$ msec, and $\tau_2 = 2$ sec. Then, when the input duration is increased, the slow process will gain in amplitude by 0.91 log unit, while the fast process will only gain by 0.47 log unit.

When the flash is extended from 100 msec to 1 sec, the slow process can integrate almost the entire flash, and thus can increase in size substantially. But the fast process will not be able to integrate nearly as much, because it will approach its asymptote much sooner.

This is illustrated in Fig. 15, where the responses of the two processes are shown on a logarithmic ordinate, for 100 msec and 1 sec inputs. The system's output is the sum of the two exponentials, and so it follows the envelope of the decay curves, with a smooth transition across the intersection.

To test the prediction of equation 4, two afterimage latency experiments were run, one using 100 msec flashes (both background and test), and the other using 1 second flashes (both background and test).

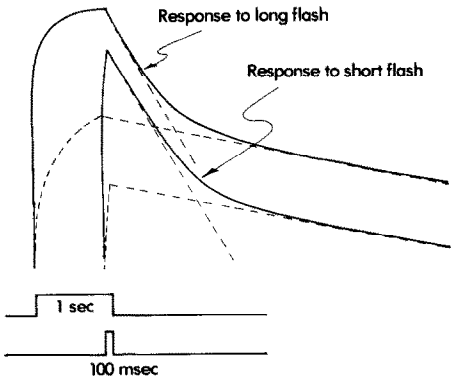

Fig. 15. The responses of a double exponential system to 100 msec and 1 sec flashes. The two exponential components, which appear as straight lines here, will each give greater responses to the longer flash. However, the slow component will integrate the longer input more effectively than will the fast component, and so will be shifted by a greater amount.

Methods

The procedure was similar to that of experiment 4. The background was red-orange (Wratten No. 24), except for background intensities above 3 log scot. td, for which it was orange (Wratten No. 22; scotopic mean wavelength 580 nm). The test was green (Ilford No. 624).

Results

Figure 16 shows the resulting latency data, for both the short flashes (solid circles), and the long flashes (open circles). The latency in this figure is plotted as time *after the offset* of the stimulus, to allow the two decay functions to line up at $t = 0$.

To interpret the results, the 100 msec data were fit with two exponentials ($\tau = 0.26$ and $\tau = 1.6$), corresponding to the two legs of the curve. By equation 4, lengthening the flash to 1 sec should shift each leg leftward along the abscissa, by an amount equal to

$$r = \log\left[\frac{1 - \exp(-1/\tau)}{1 - \exp(-0.1/\tau)}\right]. \qquad (5)$$

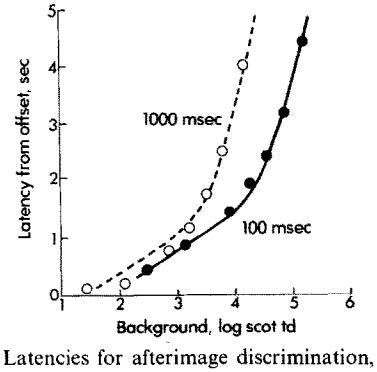

Fig. 16. Latencies for afterimage discrimination, following flashes of 100 msec (solid circles) and 1 sec (open circles). The 100 msec data were fit with a double-exponential curve (solid line), and then the corresponding results for 1 sec flashes were predicted (dashed line). Subject E.A.

This came to 0.48 log unit for the fast process ($\tau = 0.26$), and 0.88 log unit for the slow process ($\tau = 1.6$). The fit is quite good for the slow process, and fairly good for the fast process, although the data points fall somewhat below the latter curve. This last effect may be due to gain changes occurring during the 1 sec flash; a turning down of gain would cause the decaying signal to enter the linear region on the saturation curve more quickly, and so become discriminable earlier (the effect would be much less pronounced when applied to the latencies on the slow decay portion of the curve, since they would have experienced 1 or 2 sec of adaptation before becoming visible even in the short flash case).

Correlation with the physiology

The models proposed here involve a linear system which gives the persistence, and a non-linear compression which gives the saturation. It is tempting to put all the machinery into the rod itself: the internal transmitter level would exhibit the linear impulse response, and the resulting rod response would show the saturation at the level of the rod photovoltage or photocurrent. On the other hand, it remains possible that processes *beyond* the rod are responsible for both the persistence and the saturation.

To test the plausibility of this idea, we can turn to the small amount of evidence that exists on mammalian rod responses.

It is possible to extract some quantitative predictions from Penn and Hagins' (1972) recordings of rat rod photocurrent. Taking the time at which the photocurrent has fallen to halfway between the ceiling and the floor as the moment of maximum discriminability in the afterimage, one can derive a few data points on the "afterimage" latency in rat rods.

In addition, Steinberg (1969) shows some very nice recordings from horizontal cells in cat, in which he observed a persisting rod response that he termed the "rod aftereffect". His published records, with the same assumption about discrimination, also allow a prediction of the results of a rod afterimage experiment in cat.

The inferred data from Penn and Hagins, as well as those from Steinberg, are shown in Fig. 17 as solid symbols (for the data point corresponding to Steinberg's highest intensity, the published records do not show the entire response, and so it was necessary to interpolate between the visible portion and the time at which Steinberg reports that the response returned to baseline). For comparison, the human data from the present study are shown in open symbols. All of these data have been equated, as nearly as possible, to the same absolute scale of equivalent human scotopic troland seconds. Steinberg reports the intensity of his lights in terms of an estimate of percent rhodopsin bleached, which has been converted here using the equation for bleaching kinetics in human

$$\frac{dp}{dt} = I\,10^{-6.95} \qquad (6)$$

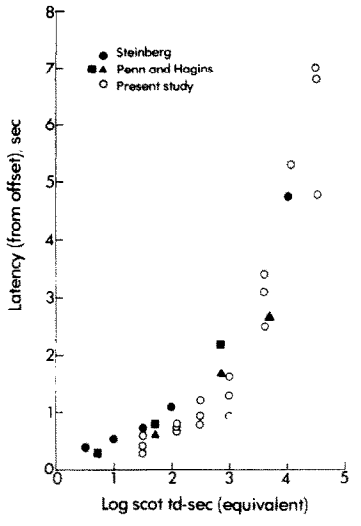

Fig. 17. Comparisons of the human delayed afterimage latencies (open circles) with predictions derived from mammalian electrophysiology (solid symbols). See text.

where p is the fraction of unbleached rhodopsin, and I is the intensity of the light in scotopic trolands (Rushton, 1956; Alpern, 1971). (Steinberg used these human kinetics, corrected for the cat's optics and tapetal reflectance, since cat kinetics were not yet known—see Bonds and MacLeod, 1974). Penn and Hagins reported their intensities in quanta absorbed per rod per flash, which has been converted to equivalent human scot. td-sec by assuming that 1 scot. td-sec leads to the absorption of 6 quanta per rod (Westheimer, 1966; Alpern and Pugh, 1974).

The agreement between these data is remarkable, given the difficulties involved in absolute light calibration, and the fact that the experiments used different species in different experimental conditions. On the basis of this comparison, there is no reason to abandon the notion that the human afterimage effects are due to processes at, or very near to, the rod photoreceptors.

In fact, the addition of persisting processes beyond the rod, or the imposition of a post-receptoral bottleneck that saturated at lower light levels than did the rod, would lead to the prediction that the human afterimage latencies would be longer, and would rise at lower light levels, than would the "afterimages" measured electrophysiologically. The actual discrepancy between the human and animal data is slightly in the other direction.

Modifying the double exponential model

The double exponential model, with fixed saturation and discrimination, works rather well. But some of the assumptions are unlikely to be strictly correct.

First of all, the model assumes that discrimination occurs when the "difference" between the two afterimage regions (i.e. the value of the comparison function) reaches some criterion value. But in a realistic model, if the criterion level is touched only briefly (say, for 1 msec), no detection will occur because the detection process involves some temporal integration (see Rashbass, 1970). Similarly, if the signal rises to this fixed level very slowly, it may not lead to detection because the afterimage behaves as a stabilized image. The problem is the same in either case: the signals that emerge from the retina are not sufficient for detection by themselves; they must pass through later machinery, and this later machinery may have both low-pass and high-pass filtering properties.

The integration associated with detection will prevent the discrimination of difference responses that are very brief. This speaks to a problem that showed itself earlier: the fact that the model predicted a very short moment of discriminability in the initial image, during the rising phase of the response (cf. Geisler, 1980).

This is illustrated in figure 18a, which shows the difference signal resulting from a saturating background and test flash. The brief initial spike reaches the same height as does the later hump, but it will have little effect on discrimination due to its brevity. Even a small amount of low-pass filtering at later stages will prevent it from reaching threshold, as shown in Fig. 18(b).

The image stabilization effect, on the other hand, will make it difficult to see extremely slow signals, such as those that occur in the afterimages following very bright flashes. These afterimages may become discriminable only after several seconds, and may rise and decay rather slowly. Figure 18(c) shows the difference response for such a slow afterimage, and Fig. 18(d) shows the effects of high pass filtering: these very slow responses should become more difficult to see.

A good quantitative theory of fading under stabilization does not yet exist, so one can only make qualitative predictions about the effects such fading will have on delayed afterimage discrimination. Stabilized images seem to fade with a time constant of about

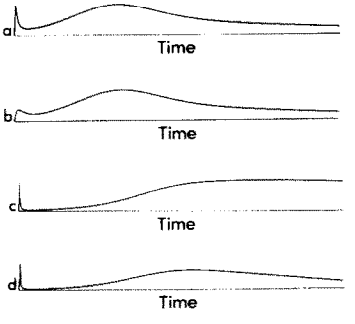

Fig. 18. The effects of high pass and low pass filtering on the detection of difference responses. (a) and (b): low-pass filtering will prevent detection of the brief initial difference that the model indicates will exist at the very beginning of the response. (c) and (d): high-pass filtering (e.g. image stabilization effects) will make it more difficult to detect the afterimages that change very slowly.

1–3 sec (Yarbus, 1967), so one could expect that afterimages which rose and fell over such periods of time would become less easily discriminable. Therefore one would predict that the Weber fraction would increase when the afterimages were appearing and disappearing over periods of a few seconds. From Figs 8 and 10, this effect should show itself at flash intensities above 3 log scot. td-sec; and Fig. 7 does in fact show an upward deviation from the Weber line above this intensity.

In general terms, then, the increment thresholds are consistent with the existence of stabilized fading effects, as well as with the slight integration associated with detection.

There is a more serious difficulty with the model as it now stands; it involves no adaptation. There is evidence that the rod system does show adaptation in similar conditions, notably a large change in gain prior to the saturating stage (Adelson, 1982). This would mean that the processes preceding saturation are quite non-linear, and so the elegant mathematics of theorems 1 and 2 should not apply. How can it be that the models derived using these theorems work so well, if the assumptions are not correct? Let us consider how gain changes will affect increment threshold and latencies for afterimage discrimination.

Increment thresholds will continue to show Weber's law under several kinds of gain change (see the appendix for a more formal discussion). If the gains in both the background and the test regions are turned down by equal amounts (which one may expect to be nearly true, since the two regions are not very different in intensity), then Weber's law will continue to hold. Moreover, if the two gains are turned down in a certain ratio to one another, and if this ratio is determined by the ratio of the intensities of the background and test regions (but not by their absolute intensities), then Weber's law will still hold. This condition is clearly satisfied when the input ratio is unity, and since the actual input ratio is near to unity, the gain ratios cannot be far from unity, or far from one another. Thus, one would not expect large disruptions of Weber's law under ordinary conditions of changing gain.

On the other hand, latency data will not emerge equally unscathed by pre-saturating gain changes. Suppose the gain has been reduced by a factor of 10 at the time of afterimage discrimination. Then the measured latency will be the same as that which would have been observed in a system of unit gain after a flash 0.1 times as bright. Thus, the internal gain changes will distort the intensity axis of a latency plot. The extent of the distortion will depend on the extent and time course of the gain changes.

We may expect, however, that much of the gain reduction will be complete within 200 msec, and that the later changes will be much smaller and slower (Adelson, 1982; Baylor and Hodgkin, 1974). If this is so, the shape of the latency curve will be distorted very little, since all latencies are collected at times

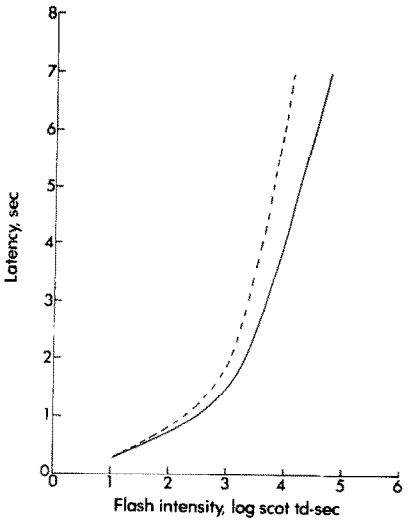

Fig. 19. The effects of a slow gain change on the latency data. Dashed line: data as they would appear with fixed gain. Solid line: distortion due to a gain change of 0.1 log unit per sec.

greater than 200 msec, after the major changes should have settled down. There will be a net shift of the curve along the intensity axis, but the shape of the curve should not be distorted.

If changes do occur, they will have effects of the sort illustrated in Fig. 19. Suppose that the gain falls by 0.1 log unit each second, so that it falls a total of 1 log unit in 10 sec. In this case, the observed latency will rise more slowly than it would have with a fixed gain. The "fixed gain" curve is shown with the dashed line. The curve that would actually be observed (solid) is somewhat distorted, but does retain the same general shape.

In summary, adaptational gain changes can be expected to have little effect on the increment threshold data, but possibly to introduce some distortion into the latency data. In neither case should the distortion be severe, and the earlier analysis in terms of non-adapting systems should remain quite useful.

SUMMARY AND CONCLUSION

When a test and background are simultaneously flashed to a dark-adapted eye, it is sometimes possible to make out the test in the fading positive rod afterimage, even if transient saturation made it impossible to see the test in the initial image. This effect may be interpreted in terms of the Penn and Hagins model of rod response, which consists of a chain of linear low-pass filters followed by a saturating non-linearity.

The Penn and Hagins model allows one to make two quantitative predictions about the afterimages: increment thresholds measured in the afterimage should follow Weber's law; and the latency for afterimage discrimination to occur should increase almost linearly with the log of flash intensity. The Weber's law prediction was upheld in the data, but the latency prediction did rather badly.

An improved model, inspired by the kinetics of the Baylor *et al.* model, was proposed. It consists of a linear system whose impulse response exhibits a double exponential decay, followed by a fixed saturating non-linearity. This model gives quite good fits to the afterimage latency data, and also predicts Weber's law for afterimage discrimination. The model was further tested in experiments involving flashes of different durations, and its predictions were found to hold fairly well.

As always, it is difficult to assign physiological structures to the psychophysics, but there is a surprising consistency between the decay of photocurrent in rat rods, the persistence of the "rod aftereffect" in cat horizontal cells, and the time course of rod afterimage signals inferred from the human psychophysics. When these three sets of data are directly compared on an absolute scale they agree remarkably well, suggesting that they originate in a common process—presumably the decay of signals within the rod outer segments.

Acknowledgements—This work was performed in partial fulfillment of the requirements for the degree of doctor of philosophy at the University of Michigan. The author was supported by National Institute of Mental Health training grant T32-MH14254 and by National Eye Institute grant ET00197 to M. Alpern. Dr Alpern's contribution of knowledge, advice, and laboratory facilities are gratefully acknowledged. The work has also benefitted greatly from discussions with Dr Angela Brown, Dr Carol Cicerone, Dr Daniel Green, Dr Donald Hood, Dr Wilson Geisler, and Dr David Krantz.

REFERENCES

Adelson E. H. (1977a) Transient rod saturation with moderate stepped backgrounds. Presented at the annual meeting of the Association for Research in Vision and Ophthalmology, Sarasota, FL.

Adelson E. H. (1977b) Decay of rod signals following bright flashes. *J. opt. Soc. Am.* **67,** 1427.

Adelson E. H. (1979) The kinetics of decay of saturated rod afterimages. *Invest. Ophthal. visual Sci., suppl.* **18,** p. 29.

Adelson E. H. (1982) Transient saturation and adaptation of the rod system. *Vision Res.* **22,** 1299–1312.

Aguilar M. and Stiles W. S. (1954) Saturation of the rod mechanism of the retina at high levels of illumination. *Optica Acta* **1,** 59–65.

Alpern M. (1971) Rhodopsin kinetics of the human eye. *J. Physiol.* **217,** 447–471.

Alpern M. and Barr L. (1962) Durations of the afterimages of brief light flashes and the theory of the Broca and Sulzer phenomenon. *J. opt. Soc. Am.* **52,** 219–221.

Alpern M. and Pugh E. N. Jr (1974) The density and photosensitivity of human rhodopsin in the living retina. *J. Physiol.* **237,** 341–370.

Alpern M., Rushton W. A. H. and Torii S. (1970a) The size of rod signals. *J. Physiol.* **206,** 193–208.

Alpern M., Rushton W. A. H. and Torii S. (1970b) Signals from cones. *J. Physiol.* **207,** 463–475.

Barlow H. B. and Sparrock J. M. B. (1964) The role of afterimages in dark adaptation. *Science* **144,** 1309–1314.

Baylor D. A., Hodgkin A. L. and Lamb T. D. (1974) Reconstruction of electrical responses of turtle cones to flashes and steps of light. *J. Physiol.* **242,** 759–791.

Brindley G. S. (1959) The discrimination of afterimages. *J. Physiol.* **147,** 194–203.

Brindley G. S. (1962) Two new properties of foveal afterimages and a photochemical hypothesis to explain them. *J. Physiol.* **164,** 168–179.

Brindley G. S. (1963) Afterimages. *Sci. Am.* **209,** Oct., 84–91.

Cervetto L., Pasino E. and Torre V. (1977) Electrical responses of rods in the retina of Bufo Marinus. *J. Physiol.* **267,** 17–51.

Craik K. J. W. (1940) Origin of visual afterimages. *Nature* **145,** 512.

Duke-Elder W. S. (1934) *Textbook of Ophthalmology*, Vol. 1. Mosby, St. Louis, MO.

Geisler W. S. (1975) Visual adaptation and inhibition. Doctoral dissertation, Indiana University.

Geisler W. S. (1980) Increment threshold and detection latency in the rod and cone systems. *Vision Res.* **20,** 981–994.

Gosline C. J., MacLeod D. I. A. and Rushton W. A. H. (1976) The dark adaptation curve of rods measured by their afterimage. *J. Physiol.* **259,** 491–499.

Hagins W. A., Penn R. D. and Yoshikami S. (1970) Dark current and photocurrent in retinal rods. *Biophys. J.* **10,** 380–412.

Hayhoe M. M., MacLeod D. I. A. and Bruch T. A. (1976) Rod-cone independence in dark adaptation. *Vision Res.* **16,** 591–600.

Helmholtz H. von (1924) *Physiological Optics* (Translated by Southall J. P. C.), Vol. 2, p. 230. Optical Society of America.

MacLeod D. I. A. and Hayhoe M. M. (1974) Rod origin or prolonged afterimages. *Science* **185,** 1171–1172.

Penn R. D. and Hagins W. A. (1972) Kinetics of the photocurrent of retinal rods. *Biophys. J.* **12,** 1073–1094.

Rashbass C. (1970) The visibility of transient changes in luminance. *J. Physiol.* **210,** 165–186.

Rushton W. A. H. (1956) The difference spectrum and the photosensitivity of rhodopsin in the living human eye. *J. Physiol.* **134,** 11–29.

Sakitt B. (1976) Psychophysical correlates of photoreceptor activity. *Vision Res.* **16,** 129–140.

Sperling G. (1960) Negative afterimage without prior positive image. *Science* **131,** 1613–1614.

Steinberg R. H. (1969) The rod after-effect in S-potentials from the cat retina. *Vision Res.* **9,** 1345–1355.

Stiles W. S. (1939) The directional sensitivity of the retina and the spectral sensitivities of the rods and cones. *Proc. R. Soc. B* **127,** 64–105.

Westheimer G. (1966) The Maxwellian view. *Vision Res.* **6,** 669–682.

Wyszecki G. and Stiles W. S. (1967) *Color Science*. Wiley, New York.

Yarbus A. L. (1967) *Eye Movements and Vision* (Translated by Basil Haigh B.) Plenum Press, New York.

APPENDIX

Mathematics of afterimage discrimination

Consider the system shown in Fig. 20. Impulse inputs enter at the left. I_1 is the intensity of a brief background flash; I_2 is the intensity of the test + background flash.

The first stage is linear, with an impulse response of $H(t)$. The second stage is a saturating non-linearity; here it takes the form

$$S = R/(R + \sigma). \tag{7}$$

Finally, the two outputs, S_1 and S_2, are compared by a discrimination box. Here, the discrimination takes the form of a simple differencing

$$D = S_2 - S_1. \tag{8}$$

Detection of the difference occurs if D exceeds some criterion value.

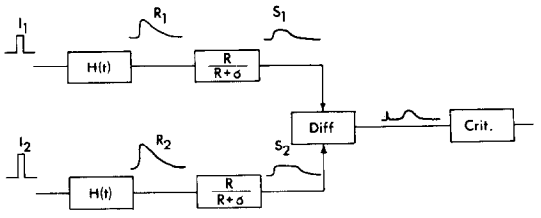

Fig. 20. Diagram of a typical L-S-D system. Two adjacent regions of the retina receive inputs of two intensities (I_1 and I_2), leading to two linear responses (R_1 and R_2), which pass through a saturating non-linearity to become S_1 and S_2. These are then compared, and if the difference is sufficiently great, detection occurs.

A system of this sort—where the saturation and discrimination functions may be quite general—will be called an "L-S-D" system (linear impulse response, with fixed saturation and discrimination functions).

Theorem 1 states that an L-S-D system must give Weber's law for afterimage discrimination. Before proceeding to the general case, it is useful to consider the concrete example for Fig. 20, where the saturation and discrimination functions have been specified (although the impulse response has been left general).

Let the inputs be in the ratio k

$$k = \frac{I_2}{I_1}. \tag{9}$$

Then, by linearity

$$\frac{R_2(t)}{R_1(t)} = k. \tag{10}$$

Following an input, R_1 and R_2 will trace out their respective responses over time, but at every instant they will be related to one another by the factor k.

S_1 and S_2 will not be related to each other by a fixed scale factor, because they are non-linear. However, there is a function that does relate them at any instant. Since

$$S_1 = \frac{R_1}{R_1 + \sigma} \tag{11}$$

and

$$S_2 = \frac{R_2}{R_2 + \sigma} \tag{12}$$

we have

$$\frac{1}{S_2} = 1 + \frac{(1 - S_1)}{kS_1}. \tag{13}$$

Observe that the relationship involves no reference to the shape of the impulse response, or the strengths of the inputs (only their ratio).

Since D is the difference of S_1 and S_2, it too is determined only by the input ratio and the instantaneous value of one response. Indeed

$$D = \frac{kR_1}{(1 + kR_1)} - \frac{R_1}{(1 + R_1)}. \tag{14}$$

The maximum value that D can attain as R_1 decays can be determined by differentiating with respect to R_1 and setting the derivative to zero. The solution is

$$1 - kR_1^2 = 0 \tag{15}$$

i.e. if the value of R_1 giving peak discriminability is called R_1^*, then

$$R_1^* = \sqrt{1/k}. \tag{16}$$

The maximum value D will attain (denoted D^*) will thus be

$$D^* = \frac{k - 1}{(1 + \sqrt{k})^2}. \tag{17}$$

The point is that the size of D^* (the peak discriminability) is entirely independent of the particular flash intensities chosen, or of the time-course of the responses. It depends only on the input ratio, k. And this is just what one requires for Weber's law to hold for afterimage discrimination.

Observe in addition that D attains this maximum at the instant for which $R_1 = \sqrt{1/k}$, regardless of the history before or after this instant.

With this example as background, let us proceed to the more general case.

Let $H(t)$ be the impulse response of a linear system, where $H(t)$ is assumed to be non-zero and to return to zero as t approaches infinity. Let $R(t) = IH(t)$ be the response to an impulse of intensity I.

Let $S(x)$, the saturation, be a monotone function, and let $D(S_1,S_2)$, the discrimination function, be any function such that, for any ratio k, D attains a maximum value taken over all x

$$D_k^* = \max_x D[S(x),S(kx)] \tag{18}$$

where D_k^* is increasing in k. (These are simply the basic properties the system must have to accord with the phenomenology of the delayed afterimages: the discriminability must reach a peak at some point, and the value of the peak must increase as the ratio of the inputs increases.)

Let X_k^* be the value of x at which D_k^* occurs.

Theorem 1

Given an L-S-D system: for impulse inputs greater than some intensity I^*, Weber's law will hold for afterimage discrimination.

Proof:

Let the inputs be in the ratio $I_2/I_1 = k$. Then by linearity

$$R_2 = kR_1 \tag{19}$$

at all times. Now, since

$$D = D[S(R_1), S(kR_1)] \tag{20}$$

the maximum value D can possibly attain as R_1 changes is

$$D_k^* = \max_x D[S(x), S(kx)]. \tag{21}$$

This value will be attained at some point during the decay of R_1 if the input I_1 was sufficiently bright; it must exceed I^*, which is the lowest value of I_1 for which the peak of R_1 reaches the value of X_k^*.

All inputs that lead to this peak will be equally discriminable; increasing the input ratio will lead to better discriminability, and vice versa. Thus, if I_1 is greater than or equal to I^*, all afterimages with a given discriminability will be generated by input pairs in a given ratio. Thus Weber's law will hold.

Theorem 2

Given an L-S-D system: if one plots the impulse response of the linear stage on semi-logarithmic coordinates, and if one similarly plots the value of flash intensity at which a given afterimage latency is obtained (with fixed k), these two curves will have the same shape, except for a change in sign and a shift along the ordinate.

Proof:

It was shown above that peak discrimination in the afterimage occurs when the response R_1 passes through some value $R_1^* = X_k^*$, which is determined only by the ratio $R_2/R_1 = k$. Thus, the latency to peak discriminability is actually the latency for R_1 to reach R_1^*.

Suppose that an input intensity of I' gives a latency of T'. We know that

$$R'(t) = I'H(t) \tag{22}$$

so that

$$R'(T') = I'H(T') \tag{23}$$

but we have defined

$$R'(T') = R_1^* \tag{24}$$

so that

$$H(T') = \frac{R_1^*}{I'}. \tag{25}$$

Thus, the intensity I', which produces a latency of T', is inversely proportional to the value of the impulse response at the instant T'. Thus, when plotted on a logarithmic ordinate, the impulse response vs time curve and the input intensity vs latency curve will have the same shape, except for a change in sign due to the inversion, and a shift due to the constant R_1^*.

Theorems 1 and 2 were derived for impulse inputs. They can be easily extended to inputs of arbitrary time-course, as long as both test and background have the same time course. One can restate the arguments above, substituting "input" for "impulse input", and "response" for "impulse response". Alternately, the following argument can be made:

Let the flash input have waveform $IW(t)$, where I is the intensity, and $W(t)$ describes the time-course of the stimulus. Let the linear stage of the L-S-D system have impulse response $H(t)$. Then the system's response to the input will be identical to the impulse response of a different linear system, whose first stage has impulse response $G(t)$, where $G(t)$ is the convolution of $W(t)$ and $H(t)$. Since this new system is also an L-S-D system, theorems 1 and 2 continue to hold for it.

Theorem 1 will also continue to apply under certain kinds of gain change. Suppose that R_1 and R_2 are both multiplied by the same gain, g. Then one can repeat the arguments of theorem 1, substituting "gR_1" for "R_1" and "gR_2" for "R_2" at every point. The theorem depends on the fact that $R_2/R_1 = k$ at every point, but since $gR_2/gR_1 = k$ as well, the arguments are unchanged. This is true even if g varies with time.

Now suppose that the gains in the two regions are not identical, but are in a fixed ratio as long as the stimulus lights are in a fixed ratio. If $g_2/g_1 = q$, then $g_2R_2/g_1R_1 = kq$. Thus, the two responses are no longer in the ratio k, but instead are in the ratio kq. But q was assumed to depend only on k, so that if k is constant, so is kq. Therefore, the responses are again always in a fixed ratio when the inputs are in a fixed ratio, and the reasoning of theorem 1 continues to apply.